Received: 21 March 2020 | Revised: 10 May 2020 | Accepted: 18 May 2020

DOI: 10.1002/elsc.202000017

Engineering in Life Sciences

RESEARCH ARTICLE

Comparison of L-tyrosine containing dipeptides reveals maximum ATP availability for L-prolyl-L-tyrosine in CHO cells

Natascha Verhagen[1] | **Andy Wiranata Wijaya**[1] | **Attila Teleki**[1] | **Muhammad Fadhlullah**[1] | **Andreas Unsöld**[2] | **Martin Schilling**[3] | **Christoph Heinrich**[4] | **Ralf Takors**[1]

[1] Institute of Biochemical Engineering, University of Stuttgart, Stuttgart, Germany

[2] Boehringer Ingelheim Pharma GmbH & Co. KG, Biberach, Germany

[3] Evonik Nutrition and Care GmbH, Darmstadt, Germany

[4] Xell AG, Bielefeld, Germany

Correspondence
Prof. Dr.-Ing Ralf Takors, University of Stuttgart, Institute of Biochemical Engineering, Allmandring 31, 70563 Stuttgart, Germany.
Email: ralf.takors@ibvt.uni-stuttgart.de

Funding information
Bundesministerium für Bildung und Forschung (BMBF), Grant/Award Number: 031L0077A

Abstract

Increasing markets for biopharmaceuticals, including monoclonal antibodies, have triggered a permanent need for bioprocess optimization. Biochemical engineering approaches often include the optimization of basal and feed media to improve productivities of Chinese hamster ovary (CHO) cell cultures. Often, L-tyrosine is added as dipeptide to deal with its poor solubility at neutral pH. Showcasing IgG1 production with CHO cells, we investigated the supplementation of three L-tyrosine (TYR, Y) containing dipeptides: glycyl-L-tyrosine (GY), L-tyrosyl-L-valine (YV), and L-prolyl-L-tyrosine (PY). While GY and YV led to almost no phenotypic and metabolic differences compared to reference samples, PY significantly amplified TYR uptake thus maximizing related catabolic activity. Consequently, ATP formation was roughly four times higher upon PY application than in reference samples.

KEYWORDS
dipeptides, flux balance analysis, CHO, media optimization, monoclonal antibody

1 | INTRODUCTION

Chinese hamster ovary (CHO) cells are important hosts for recombinant protein production and are the preferred system for monoclonal antibody production [1]. Early bioprocesses relied on the use of animal-derived sera like FBS to meet the growth and productivity needs of those cells [2]. However, the use of such sera is no longer favored because of the inherent risk of viral contamination [3] and typically high lot-to-lot variations, potentially affecting bioprocess performance and product quality [4,5].

Chemically defined (CD) media were introduced about five decades ago and predominately consisted of essential L-amino acids (Eagle's media [6]; F12 media [7]). At a concentration of about 2 mg/mL in water at room temperature and neutral pH, L-tyrosine (TYR) has the lowest solubility of all essential amino acids. Accordingly, only small amounts of TYR can be added to basal and feed media

Abbreviations: CAC, citric acid cycle; CHO, Chinese hamster ovary; EMP, Embden-Meyerhof Parnas; FBA, flux balance analysis; GY, glycyl-L-tyrosine; mAB, monoclonal antibody; MAS, malate-aspartate shuttle; NADH, nicotinamide adenine dinucleotide; PY, L-prolyl-L-tyrosine; REF, reference; TYR, L-tyrosine; VCD, viable cell density; YV, L-tyrosyl-L-valine

to avoid unwanted media precipitation, thereby trying to ensure process stability [5]. Non-wanted TYR insolubility could be prevented by feeding TYR with high pH because the latter greatly increases TYR solubility. However, pH control, salt concentration, and precipitation in the bioreactor are potential problems that can occur with such an approach. A safer and more robust approach is the replacement of single TYR by TYR-containing, chemically defined dipeptides, which can increase solubility up to 250-fold at neutral pH [8].

The industrial performance of CHO cells using specific TYR dipeptides was examined by Kang et al. [5], who demonstrated that substituting free amino acids with L-tyrosyl-L-lysine (YK), L-tyrosyl-L-histidine (LH), L-tyrosyl-L-alanine (YA), and L-tyrosyl-L-valine (YV) decreased secretion of lactate and ammonium by-products. Sánchez-Kopper et al. (2016) [9] showed that dipeptides such as L-alanyl-L-tyrosine (AY), glycyl-L-tyrosine (GY), and L-prolyl-L-tyrosine (PY) are taken up by CHO cells and cleaved intracellularly before entering catabolic and anabolic pathways. Furthermore, recent patents [10] demonstrate industrial interest in protecting the use of TYR-containing dipeptides in feed media.

In this study, we focus on the use of TYR-dipeptides as additional feeding compounds. We investigated the impact of related dipeptides on cellular metabolism. While the potential of TYR-containing dipeptides has been shown by the above studies, little is known about the metabolic consequences resulting from their consumption. Showcasing IgG1 production with CHO cells, our investigation focused on the metabolic impact of dipeptide bolus feeding. We chose GY, YV, and PY as our model dipeptides. Phenotypic tests were complemented by quantitative metabolomics and flux analysis to decipher differences caused by dipeptides compared to cells lacking dipeptides in their feed. Whereas GY and YV did not significantly alter metabolism, PY increased the ATP supply, which represents a promising optimization target for future studies.

PRACTICAL APPLICATION

L-Tyrosine (TYR) is an essential amino acid for mammalian cells and shows poor solubility in cell culture media at neutral pH. Accordingly, TYR-containing dipeptides are commonly used that offer improved cellular supply. Here, we investigate the application of three L-tyrosine containing dipeptides showcasing the production of IgG1 with Chinese hamster ovary (CHO) cells. L-Prolyl-L-tyrosine (PY) caused the highest intracellular ATP availability that is an important property for all experimentalists in this field.

2 | MATERIALS AND METHODS

2.1 | Seed train, shake flask cultivation, and addition of dipeptides

The following dipeptides containing TYR were supplied by Evonik Nutrition and Care GmbH (Darmstadt, Germany): glycyl-L-tyrosine (GY), L-prolyl-L-tyrosine (PY), and L-tyrosyl-L-valine (YV). The IgG1-producing CHO suspension cell line BIBH1 (provided by Boehringer Ingelheim Pharma GmbH & Co. KG, Biberach, Germany) was grown in chemically defined TC-42 medium (Xell AG, Bielefeld, Germany) supplemented with 4 mM L-glutamine (Carl Roth GmbH & Co. KG, Karlsruhe, Germany), 200 nM methotrexate (Sigma–Aldrich, Steinheim, Germany), and 0.1 g/L geneticin (Fisher-Scientific, Schwerte, Germany). Seed train and experiments were performed in pre-sterilized disposable shake flasks (Corning Inc., New York, USA) in a humidified and incubated rotary shaker (Infors HT Minitron, Infors GmbH, Einsbach, Germany) at 37°C, 150 rpm with 50 mm displacement, and 5% CO_2. Stock solutions of TYR-based dipeptides were solved at neutral pH and introduced at the beginning of cultivation (0.05 mM). Furthermore, daily additions (0.05 mmol) of dipeptides were performed from 48 to 120 h of cultivation. In reference cell cultures, sterilized water was used to mimic the additional liquid volume in experimental cultures. Cultivation was performed with biological duplicates in two independent experiments.

2.2 | Extracellular analysis

Samples were taken at least once a day during cultivation. Viable cell density and viability were determined using trypan blue staining and a Cedex XS cell counter (Innovatis AG, Bielefeld, Germany). The extracellular concentrations of D-glucose (D-glc) and L-lactate (L-lac) were determined using a Labotrace automatic analyzer (Trace Analytics GmbH, Braunschweig, Germany). The concentration of produced IgG was determined with an ELISA [11]. All sampling and measurement procedures were performed with three technical replicates. The extracellular concentrations of all proteinogenic amino acids with the exception of L-cysteine were quantified using reversed-phase chromatography (Agilent 1200 Series, Agilent Technologies, Waldbronn, Ger-

many) with a precolumn fluorometric derivatization step using ortho-phthaldiealdehyde (OPA)/9-fluorenylmethyl chloroformate (FMOC) [12,13]. The internal standard γ-aminobutyric acid (GABA) was added to all standard-based external calibration levels and the analyzed samples.

2.3 | Intracellular analysis

For each intracellular sample, 1.6×10^7 cells were harvested, gently centrifuged (10 min, $300 \times g$, 4°C), washed, and quenched in liquid nitrogen. Washing steps were performed three times using ice-cold isotonic PBS solution to remove all extracellular compounds attached to the cells. Samples were taken after 60, 72, 76, 84, 96, 108, and 120 h of cultivation. Pre-processed cell pellets were stored at −70°C. The intracellular metabolome was extracted from defined pellets using an adapted cold methanol/chloroform extraction method [9]. An ice-cold 1:2 $CHCl_3$:MeOH solution was added to cells followed by ice-cold $CHCl_3$ solution and finally by ice-cold water, with 5 min of vortexing after each addition. Resulting suspensions were incubated for 1 h at 4°C in a rotary overhead-shaker. Phase separation was afterward achieved by centrifugation for 10 min at $3200 \times g$ and 0°C. The upper aqueous phase was separated and stored at −70°C for further analysis. Dipeptide, amino acid, and central metabolite concentrations were determined on an HPLC system (Agilent 1200 Series) coupled with an Agilent 6410B triple quadrupole tandem mass spectrometer (QQQ-MS/MS, Agilent Technologies, Waldbronn, Germany). The LC–MS method was based on a bicratic (two-phase) zwitterionic hydrophilic interaction chromatography (ZIC-pHILIC) under alkaline mobile phase conditions without any derivatization [14,15]. Targeted metabolites were detected with high selectivity with pre-optimized precursor-to-product ion transitions and associated MS/MS settings in multiple reaction monitoring (MRM) mode. Absolute quantifications were performed by adapted standard-based external calibrations with constant addition of global internal standards (50 μM L-norvaline and GABA). Data were analyzed using MassHunter B.06.00 Analysis software.

Intracellular pools of AxP nucleotides were determined using an ion-pair-reversed-phase chromatography method with a HPLC system (Agilent 1200 Series) [16]. Underivatized samples were detected via UV light (diode array detector). Quantifications were performed by external standard calibration and selected samples were spiked with AMP, ADP, and ATP (internal calibration) to evaluate the influence of the sample matrix.

2.4 | Cell-specific rate estimations

Cell-specific rates of changes in extracellular metabolites were used as constraints when performing flux balance analysis (FBA). Cell-specific exo-metabolic rates were estimated from extracellular metabolite concentrations and viable cell density over time. Using Equations 1 and 2 and linear regression, growth rate and specific exo-metabolome uptake and secretion rates were estimated.

$$\frac{dC_X}{dt} = \mu C_x \Rightarrow \ln(C_x) = \mu(t - t_0) + \ln(C_0) \quad (1)$$

$$\frac{dC_i}{dt} = q_i C_x \Rightarrow C_i = \left(\frac{q_i}{\mu}\right) C_x - C_{i,0} \quad (2)$$

2.5 | Flux balance analysis

The metabolic model used in this study is a simplified genome-based model derived from the following sources: KEGG [17], CHOMINE [18], and *Mus musculus* GeM [19]. The detailed metabolic model is presented in Supporting Information S1. This model includes the central carbon metabolic pathway (consisting of the Embden-Meyerhof Parnas [EMP; glycolysis], pentose phosphate pathway [PPP], citric acid cycle [CAC], and anaplerotic reactions), the biosynthesis of essential biomass precursors (fatty acids, steroids, glycogen, and nucleotides), and amino acid catabolism. The biomass composition required to model cell growth uses values reported by Sheikh et al. [20], whereas antibody composition is based on Martens [21]. Dipeptide cleavage occurs intracellularly following findings reported by Sánchez-Kopper et al. [9].

FBA was used to predict the fate of intracellular dipeptides and determine their role in CHO metabolism. FBA was performed using Insilico Discovery (Insilico Biotechnology, Stuttgart, Germany). FBA was carried out during the exponential growth phase, when the highest amount of dipeptide consumption occurs. Multiple assumptions were made for FBA. First, FBA was performed under a metabolic steady state with a constant growth rate and specific rates of change in D-glucose, L-lactate, L-glutamine, and L-asparagine levels. Additionally, the P/O ratio of nicotinamide adenine dinucleotide (NADH) and flavin adenine dinucleotide ($FADH_2$) oxidation was assumed to be 1.5 and 1.2 mol ATP per mol of the nucleotide, respectively. FBA was performed using growth rate and extracellular metabolome uptake/secretion rates as constraints. The objective function of FBA was to maximize the model-predicted growth rate.

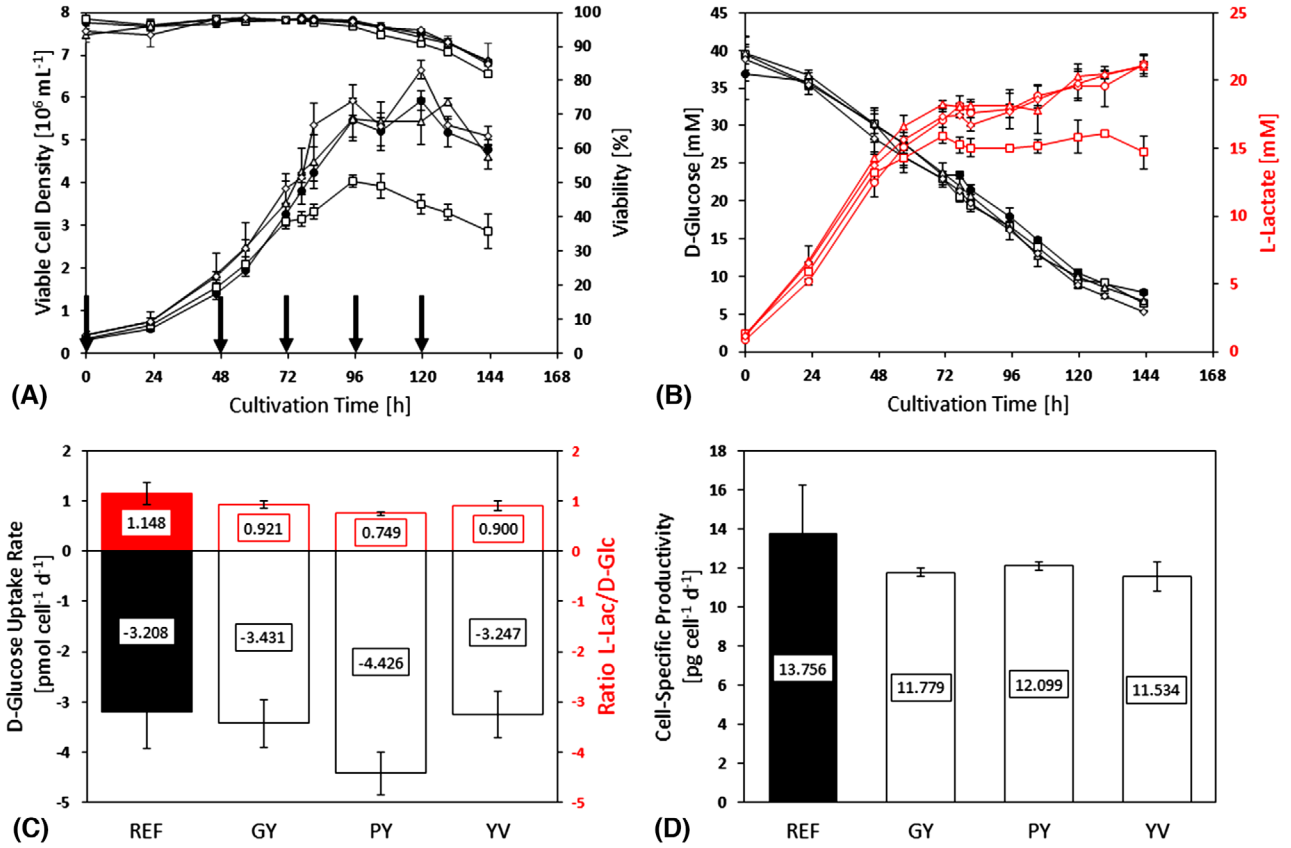

FIGURE 1 (A) Time courses of viable cell density [10^6 cells mL^{-1}] and viability [%] and (B) time courses of extracellular D-glucose (black) and L-lactate (red) concentrations [mM] of dipeptide supplemented cells (GY Δ, PY □, YV ◊) and reference (REF ●). Arrows indicate time points at which dipeptides or water were added. (C) Cell-specific rates of the exponential phase are calculated in [pmol $cell^{-1}$ d^{-1}] for D-glucose consumption (black) and D-glucose-to-L-lactate-ratio (red). (D) Cell-specific productivity [pg $cell^{-1}$ d^{-1}] of dipeptide supplemented cells (GY, PY, YV) and the reference (REF) in the exponential phase. Error bars show standard deviations of biological duplicates

Three simulations were performed for experimental and control cultures (REF, GY, PY, and YV) to obtain the maximum, minimum, and median rate predictions. Maximum (best-case scenario) and minimum predictions were simulated using the maximum or minimum uptake and secretion rates, respectively. For median estimation, maximum and minimum settings were applied as constraints. Upper and lower confidence intervals were calculated using twice the standard error of the predictions (i.e., 95% confidence level).

3 | RESULTS

3.1 | The addition of L-prolyl-L-tyrosine alters cell growth and metabolism

Initially, TYR-containing dipeptides were added to a final concentration of 0.5 mM to cell culture medium used to cultivate CHO BIBH1 cells for IgG1-antibody production. Fresh additions of TYR-containing dipeptides (0.05 mmol) took place after 48, 72, 96, and 120 h of cultivation (indicated by arrows in Figure 1). The addition of L-prolyl-L-tyrosine (PY) significantly reduced viable cell density (VCD), unlike the addition of glycyl-L-tyrosine (GY) and L-tyrosyl-L-valine (YV). Cells receiving regular additions of PY only reached a maximum viable cell density of $(4.030 \pm 0.153) \times 10^6$ cells/mL, which was approximately two-thirds of the viable cell densities of GY, YV, and reference (REF) cultures.

PY addition affected antibody titer (Supporting Information S2, Figure S1) whereas cell-specific antibody productivity was similar for all experimental conditions. Specific D-glucose consumption rates were highest after PY addition during the exponential phase. Furthermore, cells that grew in medium with PY showed reduced L-lactate formation reflected in the low ratio of D-glucose consumption to L-lactate secretion (PY: 0.749 ± 0.030 $mol_{D\text{-}Glucose}/mol_{L\text{-}Lactate}$; REF: 1.148 ± 0.161 $mol_{D\text{-}Glucose}/mol_{L\text{-}Lactate}$; Figure 1).

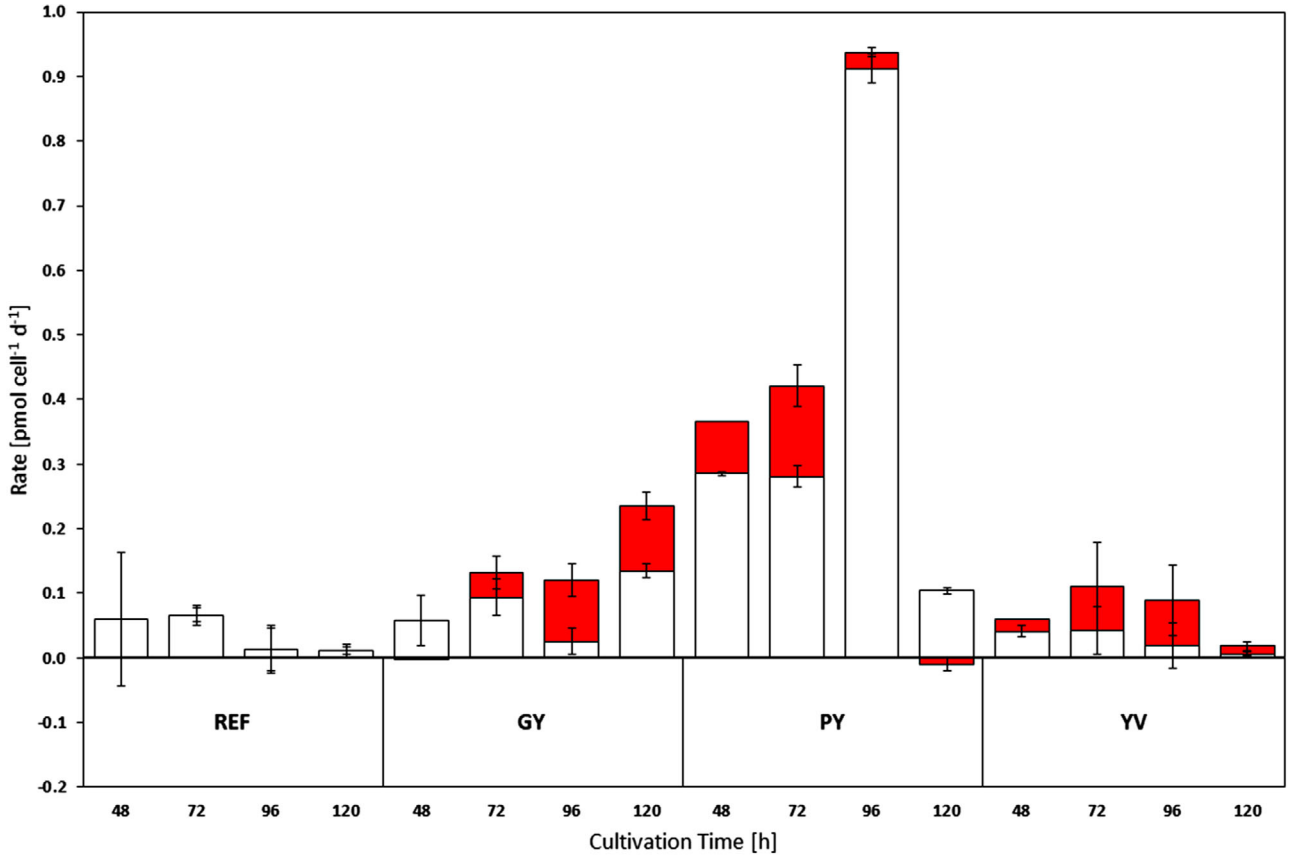

FIGURE 2 TYR uptake and release rates [pmol cell^{-1} d^{-1}] via dipeptides addition compared to reference cultures (REF) after 48, 72, 96, and 120 h of cultivation. Columns indicate the total levels of dipeptide uptake consisting of retained (white) and released (red) parts of TYR. Error bars show standard deviations of biological duplicates

3.2 | Dipeptide uptake depends on composition and causes metabolic changes

Uptake dynamics of TYR at different cultivation time points (48, 72, 96, and 120 h) are displayed in Figure 2. PY addition led to the largest total TYR uptake rates (indicated by the entire columns) and the largest fractions of TYR that remained intracellular (white columns) after 48, 72, and 96 h of cultivation. Remarkably, each addition of a TYR-containing dipeptide increased TYR uptake compared to reference cultures. However, some TYR from the decomposed dipeptide was always secreted (indicated by the red bar).

Small intracellular pools of dipeptides measured in intracellular extracts indicate the uptake of all dipeptides by cells. Intracellular fluctuations reflect extracellular bolus feeding. Repeated dipeptide addition to the medium (48, 72, 96, and 120 h) increased extracellular concentrations and consequently increased intracellular pool sizes of the intact dipeptides thereafter. Besides GY and YV, extracellular PY is depleted at 72 and 96 h demonstrating the faster uptake of PY (Supporting Information S2, Figure S2).

Uptake rates of the essential amino acid L-glutamine were similar in PY (-1.297 ± 0.047 pmol cell^{-1} d^{-1}), GY (-1.243 ± 0.170 pmol cell^{-1} d^{-1}), and REF (-1.373 ± 0.042 pmol cell^{-1} d^{-1}) conditions but differed under YV conditions (-1.028 ± 0.038 pmol cell^{-1} d^{-1}). In contrast, sizes of intracellular L-glutamine pools differed. Compared to REF cultures, YV addition increased the L-glutamine pool while GY addition diminished the L-glutamine pool and PY addition nearly depleted the L-glutamine pool (Figure 3).

As outlined in Figure 2, cells always consumed the surplus of TYR provided by dipeptide addition and retained different fractions of that TYR. The additional TYR provided by PY affected the energetic status of the cells and increased ATP pool sizes beginning from 72 h after cultivation (Figure 4). Simultaneously, AMP pool sizes decreased after dipeptide addition.

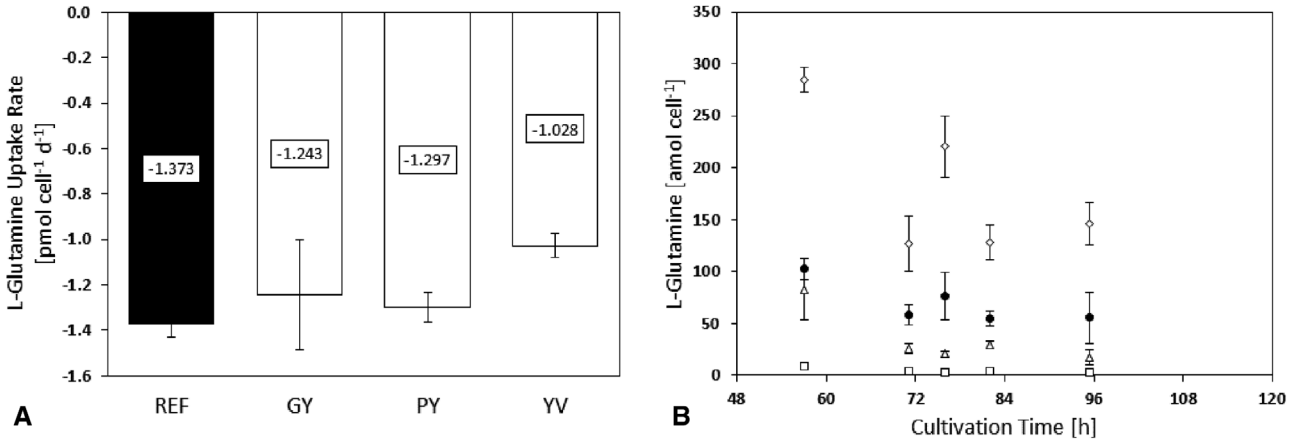

FIGURE 3 L-Glutamine consumption rates [pmol cell^{-1} d^{-1}] (A) and intracellular pool sizes [amol cell^{-1}] (B) of dipeptide-supplemented cells (GY Δ, PY □, YV ◊) and reference cells (REF ●). Negative values indicate an uptake. Error bars show standard deviations of biological duplicates

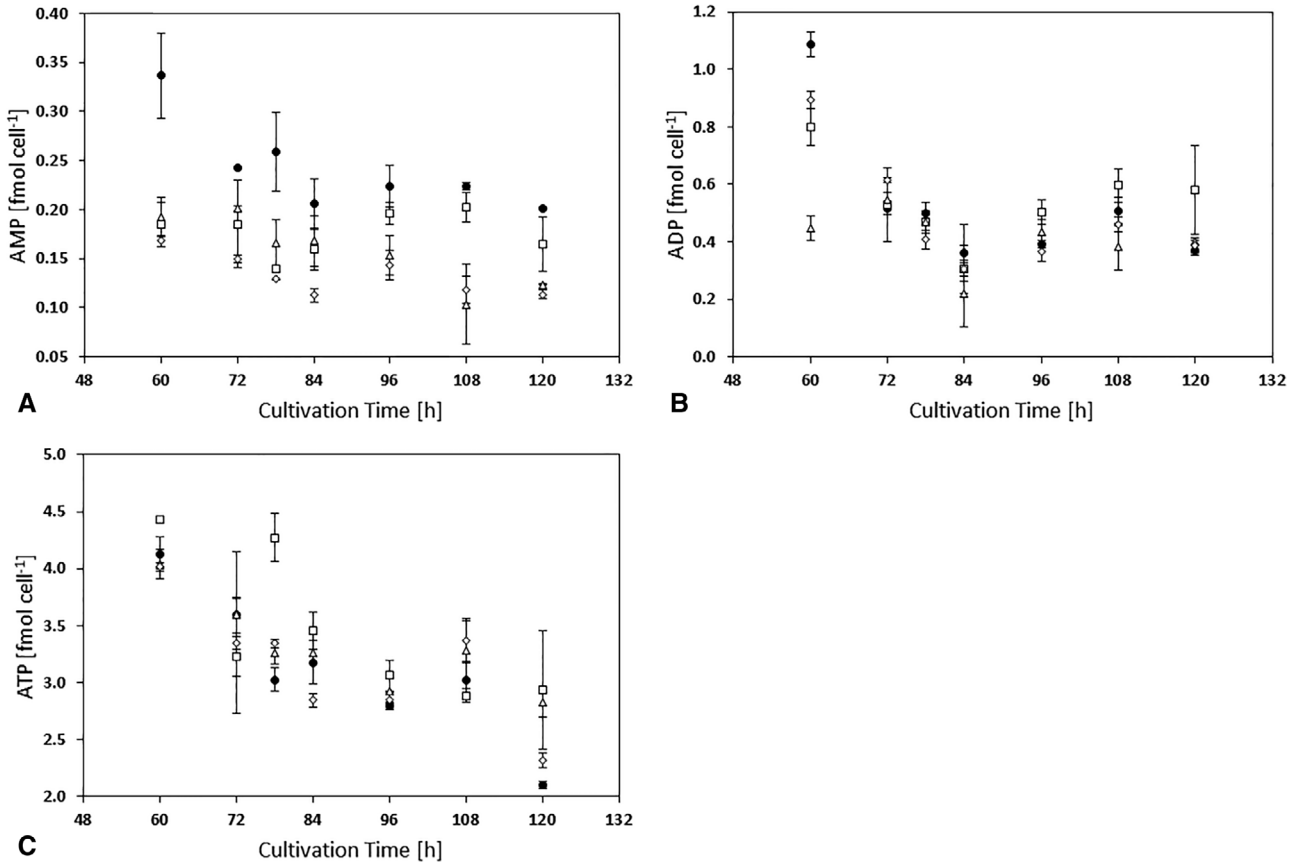

FIGURE 4 Intracellular pools of AMP (A), ADP (B), and ATP (C) [fmol cell^{-1}] of dipeptide supplemented cells (GY Δ, PY □, YV ◊) and reference cells (REF ●). Error bars show standard deviations of biological duplicates

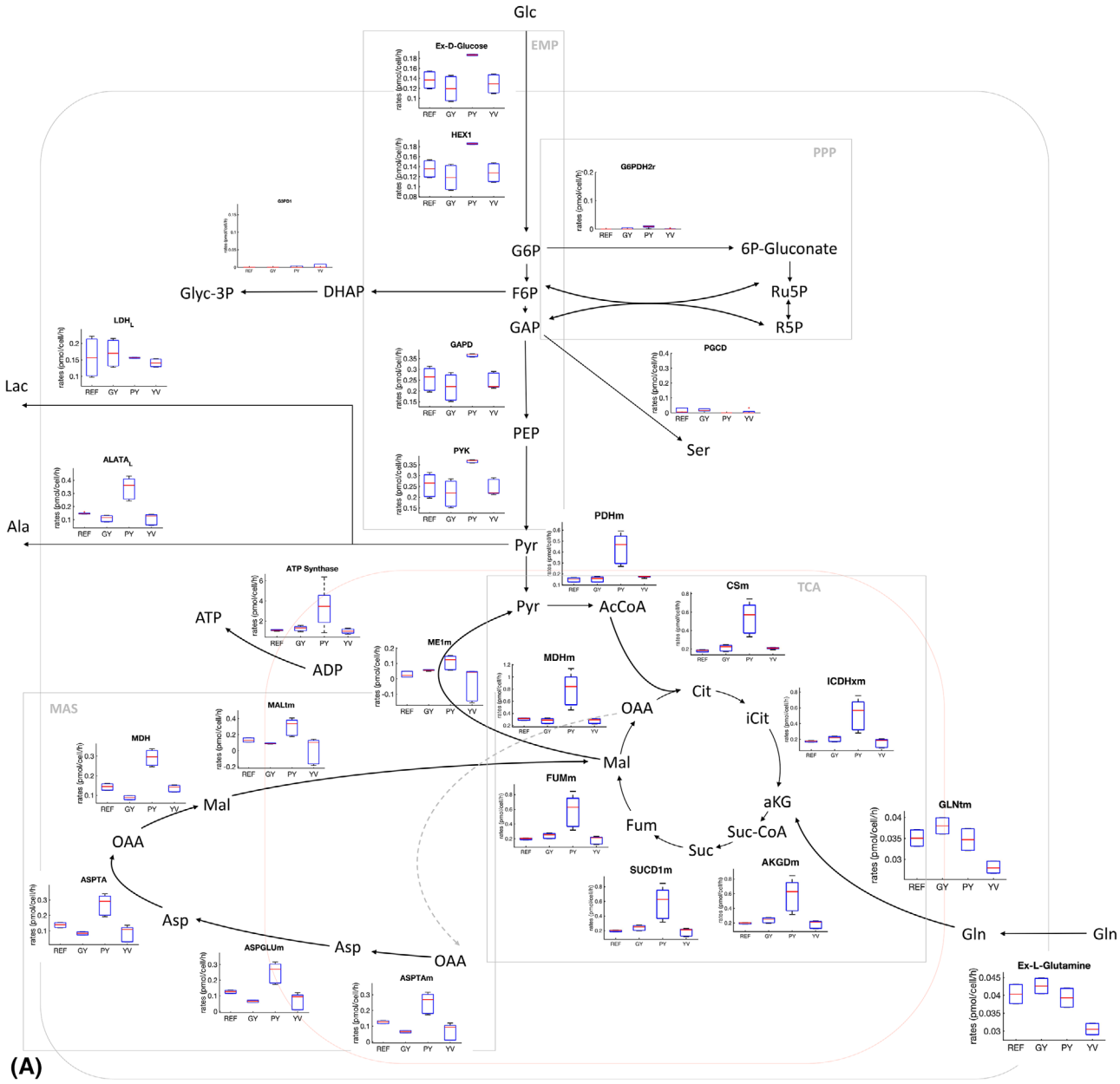

FIGURE 5 (A) Central carbon metabolism flux distribution during exponential growth phase as determined FBA. The boxplot indicates the flux of each reaction with samples arranged in the sequence REF-GY-PY-TY from left to right; (B) Cytosolic NADH production and consumption. Cytosolic NADH is produced predominantly by the EMP pathway. Additionally, NADH/NAD conversion can occur via lactate dehydrogenase (LDH) and/or the malate-aspartate shuttle (MAS). The pie chart indicates fractional amounts, not absolute amounts

3.3 | In silico analysis of the effects of TYR-containing dipeptides on metabolic activities of CHO cells

Figure 5 shows the flux distributions obtained using FBA. FBA was performed during the exponential growth phase (0–96 h of cultivation) where the TYR-containing dipeptides were supplemented to the cultures. Due to the higher D-glucose uptake rate and similar L-lactate secretion rate in PY cultures, it is expected that more glycolytic carbon was channeled to mitochondria in PY cultures compared to other cultures. The fraction of carbon diverted to the PPP, L-serine biosynthesis, and glycerophospholipid biosynthesis is negligible since cellular requirements for purine and glycerophospholipids are low. Moreover, L-serine was also available in the cultivation media.

Accordingly, the estimated citric acid cycle (CAC) flux of PY cultures was about three times higher than in the other cultures.

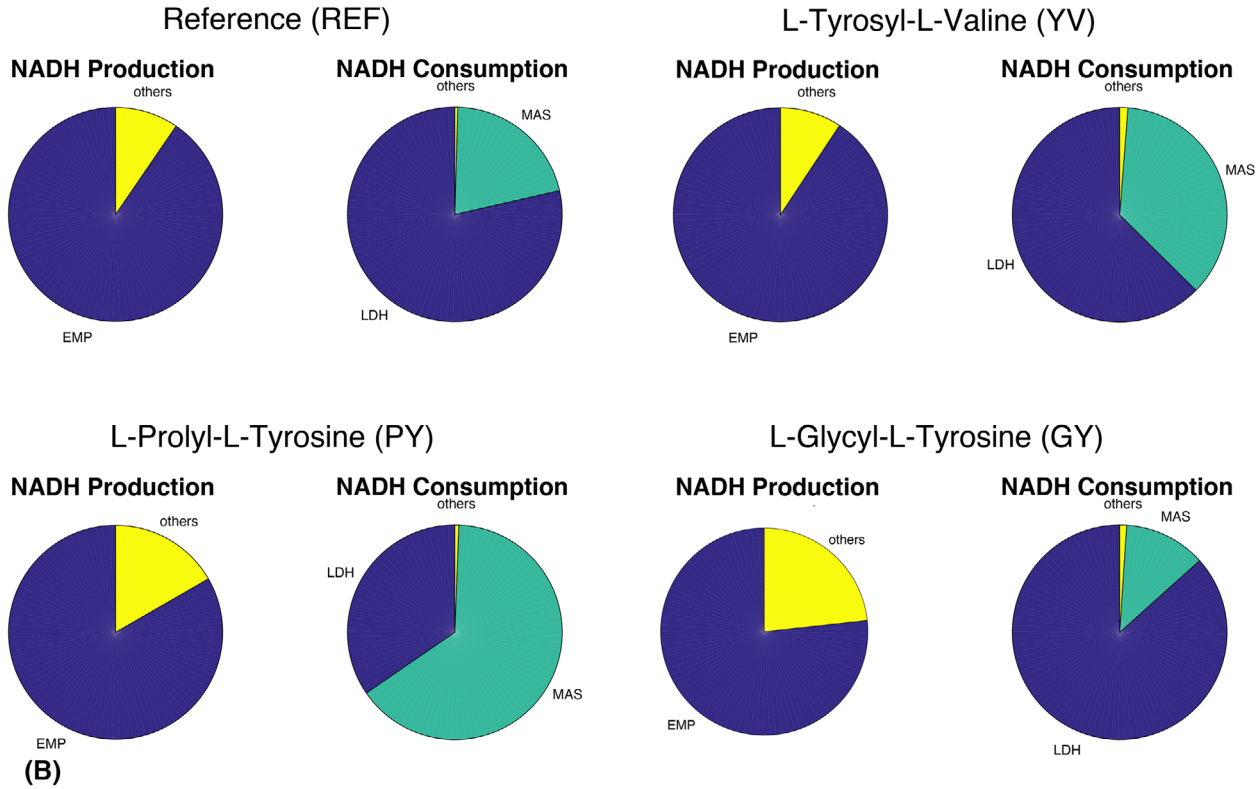

FIGURE 5 Continued

Higher glycolytic flux in PY cultures increased production of cytosolic nicotinamide adenine dinucleotide (NADH). Since the activity of NADH-consuming lactate dehydrogenase was low, NADH was transferred to mitochondria to fuel oxidative phosphorylation. NADH enters mitochondria via the malate–aspartate shuttle (MAS). In our in silico analysis (Figure 5), MAS activity in the PY cultures was 0.29 $pmol_{NADH}$ $cell^{-1}$ h^{-1} and responsible for 65% of cytosolic NADH while MAS activity in REF, YV, and GY cultures yielded 21%, 36%, and 13% cytosolic NADH, respectively. Additionally, FBA predictions revealed that incoming carbon from L-glutamine catabolism did not significantly affect the total CAC flux.

In addition to alleviated D-glucose uptake rates, PY cultures also showed elevated essential amino acid consumption (Supporting Information S2, Figure S3). Considering that cells grew at equal rates in all cultures, the increased amino acid uptake of PY cells is predicted to provide additional ATP. Different dipeptide uptake rates were observed in cultures leading to different fractions of catabolized TYR in FBA calculations (Figure 6). Figure 7 displays the correlation between TYR-containing dipeptide uptake and TYR fraction metabolism in cells. Additionally, a saturating uptake kinetic is observed, hinting at a maximum internal TYR metabolism.

4 | DISCUSSION

Dipeptides are promising supplements for cell culture media in order to compensate for low solubility and stability of individual amino acids. Previous studies have demonstrated that peptide addition may have diverse effects on cellular performance, motivating further tests to elucidate the underlying mechanisms [5,9]. The initial goal of this study was to identify TYR-containing dipeptides that can increase the maximum supply of TYR to cells through cell culture medium. Our experimental findings support the hypothesis that the metabolic effects of TYR depend on the molecular structure of the TYR-containing dipeptide. More specifically, L-prolyl-L-tyrosine (PY) alters cellular metabolism, unlike glycyl-L-tyrosine (GY) and L-tyrosyl-L-valine (YV).

The data support the potential for different uptake mechanisms and kinetics of TYR-containing dipeptides [9]. Moreover, the investigation of intracellular dipeptide pools showed that PY, GY, and YV were taken up as intact dipeptides (Supporting Information S2, Figure S2). Once they entered the cell, the dipeptides were either rapidly degraded, metabolized, or exported. Based on recent CHO genome sequencing and annotation studies, the importers PepT1 and PepT2 may be responsible for dipeptide uptake [18], however, such identification does not yet explain the dipeptide type-dependent differences.

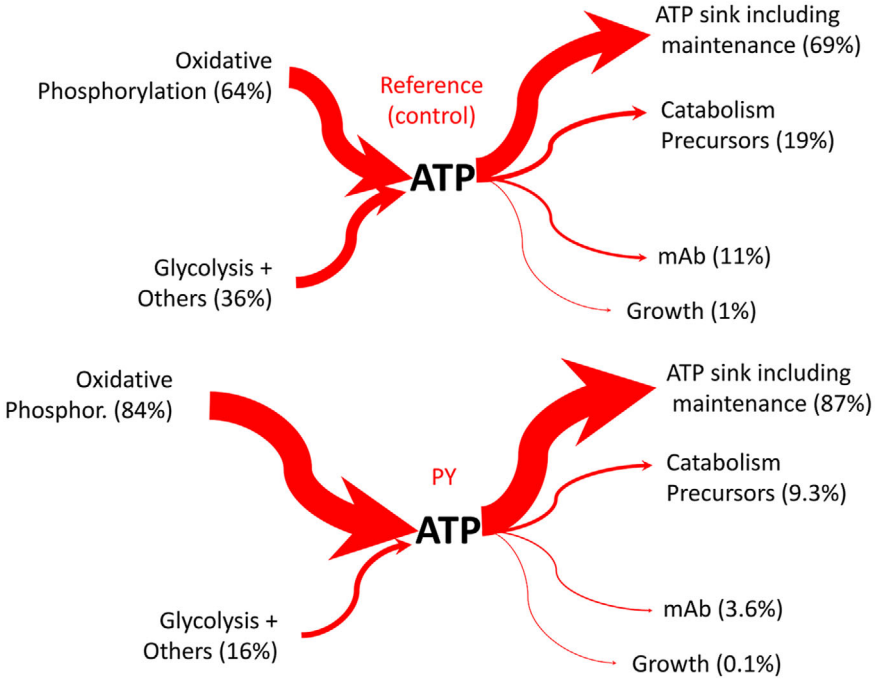

FIGURE 6 ATP flow in reference and PY cultures. The percentage indicates the portion produced or consumed by cellular metabolism

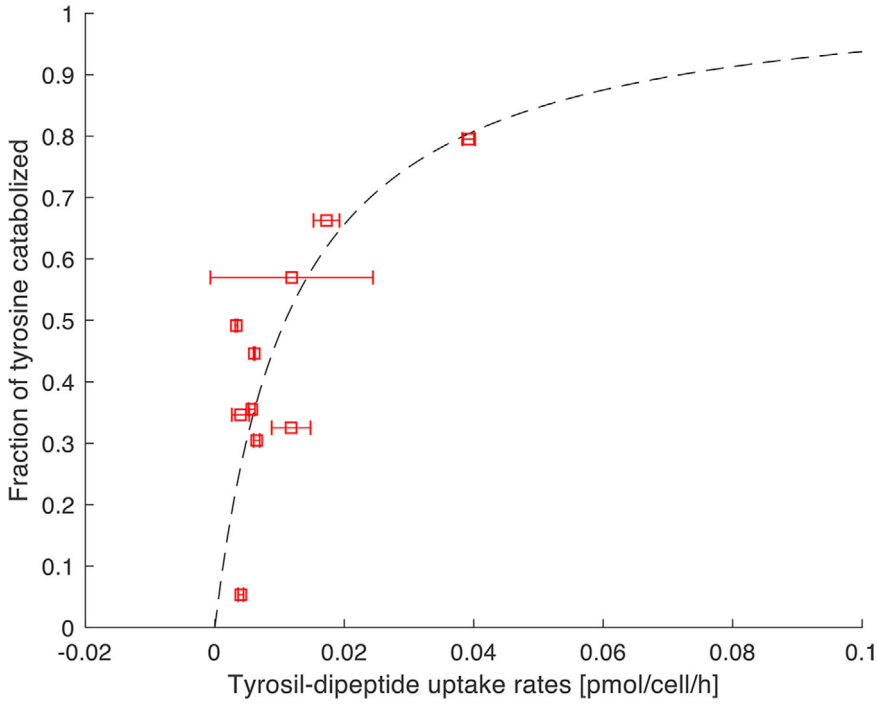

FIGURE 7 The correlation of TYR-containing dipeptides uptake rates with the fraction of TYR metabolized. This correlation forms saturating kinetics indicating that there is a maximal TYR metabolism

PY showed the strongest impact of all tested dipeptides on CHO metabolism and caused decreased growth, increased D-glucose uptake, and reduced overflow metabolism (Figure 1). Moreover, PY supplementation also altered CAC activity, intracellular ATP pools (Figure 4 and 5), and depleted the L-glutamine pool (Figure 3).

The dipeptide PY possibly works as a signal molecule (demonstrated for amino acids by Franek and Sramkova) inducing a reprogramming of the cellular metabolism [22]. An altered intracellular pH (pH_i) may contribute especially to reduced VCD and modified enzyme activities. In this experiment, our data did not encourage a changed pH_i as we observed enhanced D-glc uptake [23]. Additionally, the data set is not sufficient to reveal this effect as intracellular data of L-lac, NH_4^+, and pH_i were not applicable in this setting and were not within the scope of this study.

Nevertheless, addition of PY possibly triggers signaling pathway that contribute to decreased VCD and enhanced ATP formation.

Our FBA results suggest that CAC activity was increased in PY-treated cultures based on relatively low L-lactate formation relative to the D-glucose consumed. Moreover, D-glucose uptake rates of PY-treated cultures were approximately 30% higher compared to other cultures and mitochondrial malate-aspartate shuttle (MAS) activity was tripled in PY cultures compared to the reference (REF) culture. Such phenomenon can be interpreted as cellular responses to increased NADH supply in the cytosol while MAS activity reflects increases in glycolytic activity and reductions in L-lactate formation. MAS, a known indirect transporter of NADH from the cytosol to mitochondria, shuffles excess cytosolic NADH into the mitochondrion to fuel respiration and ATP formation. These metabolic changes resulted in an approximately four times higher ATP formation in PY culture compared to the others.

For our FBA model, only three TYR sinks are possible: (i) TYR utilization for building macromolecules like cellular proteins or mAB, (ii) TYR export, and (iii) TYR catabolism. Interestingly enough, we identified sink (iii) as the dominant fate of TYR, thus TYR was predominately used for ATP formation, beginning with its deamination using α-ketoglutarate (αKG) as amino acceptor. Next, the remaining carbon backbone is converted into fumarate and acetyl-CoA in mitochondria, thus fueling the CAC and supporting respiration. To generate sufficient αKG supply for such scenarios, one of two routes may be engaged, either through quick deamination of L-glutamate, the product of αKG amination, to create a steady-state cycle or the replenishment of αKG by the sequential deamination of L-glutamine. The observation of diminishing levels of intracellular αKG and extracellular L-glutamine pools favors the second scenario. Notably, GY and YV consumption did not result in similar trends of intracellular αKG and extracellular L-glutamine levels compared to PY consumption. Instead, upon GY or YV consumption, L-glutamine pools remained steady or were even elevated and αKG levels showed no decrease.

Becker et al. [24] demonstrated that the cell-specific mAB productivity q_{mAB} rises in D-glucose-limited perfusion cultures when ATP formation via respiration is increased [24]. However, those results are not strictly applicable to our study as our cells were analyzed under D-glucose-saturated conditions. Accordingly, our observations should be compared to those of Bulté et al. [25] who observed increased CAC activity without rising q_{mAB} [25]. Apparently, ATP supply does not limit mAB production under D-glucose-saturating conditions.

Mammalian cells are well known for their high ATP requirements to meet maintenance demands. Killburn et al. [26] estimated this ATP requirement to be larger than 65% of total ATP [26]. Consequently, D-glucose-limited cells, including those in perfusion cultures, may be in an ATP-limited condition such that an additional ATP supply fuels maintenance demands, establishes ion gradients [27] and boosts anabolic mAB formation. In contrast, D-glucose-saturated cells are likely to satisfy ATP maintenance demands, allowing for the use of excess ATP for the formation of recombinant proteins like mAB production. However, such demands are fairly low, only requiring about 11% of total ATP in the reference cultures (Figure 6). As indicated, ATP demands in reference cultures were estimated as 69% of total ATP, in line with the findings of Killburn et al. [26].

5 | CONCLUDING REMARKS

In conclusion, we demonstrated that TYR-containing dipeptides influence CHO cell metabolism in different ways depending on their specific amino acid combination. While the dipeptides glycyl-L-tyrosine (GY) and L-tyrosyl-L-valine (YV) showed minimal impact on cellular metabolism, L-prolyl-L-tyrosine (PY) increased L-glutamine usage and increased ATP availability in the cells. Strictly speaking, the FBA approach cannot distinguish between rising ATP demands for maintenance or improved ATP availability beyond what is required for maintenance. Additional ^{13}C flux studies may help to decipher the maintenance versus excess question experimentally. Our evidence of increased ATP pools in PY cultures favors the presence of improved ATP supply with unchanged maintenance demands. As next step, this exploitation potential could be used to transfer the additional energy into improved product formation. Input parameters like proper D-glucose limitation in combination with different PY feed scenarios should be tested to further optimize production performance.

NOMENCLATURE

C_i [mmol/L]	Extracellular concentration of metabolite i
C_x [cell/L]	Viable Cell Density (VCD)
q_i [pmol/cell/h]	Extracellular production/consumption rate of i
μ [h^{-1}]	cell-specific growth rate

ACKNOWLEDGMENTS

The authors gratefully acknowledge the funding by the Bundesministerium für Bildung und Forschung (BMBF), (Funding Number 031L0077A).

CONFLICT OF INTEREST

The authors have declared no conflict of interest.

ORCID

Andy Wiranata Wijaya https://orcid.org/0000-0001-9388-7357

REFERENCES

1. Birch, J. R., Racher, A. J. Antibody production. Adv. Drug. Deliv. Rev. 2006, 58, 671–685.
2. Gstraunthaler, G. Alternatives to the use of fetal bovine serum: serum-free cell culture. ALTEX Altern. Anim. Exp. 2003, 20, 275–281.
3. Wessman, S. J., Levings, R. L. Benefits and risks due to animal serum used in cell culture production. Dev. Biol. Stand. 1999, 99, 3–8.
4. van der Valk, J., Brunner, D., De Smet, K., Svenningsen, Å. F. et al. Optimization of chemically defined cell culture media–replacing fetal bovine serum in mammalian in vitro methods. Toxicol. in Vitro 2010, 24, 1053–1063.
5. Kang, S., Mullen, J., Miranda, L. P., Deshpande, R. Utilization of tyrosine-and histidine-containing dipeptides to enhance productivity and culture viability. Biotechnol. Bioeng. 2012, 109, 2286–2294.
6. Eagle, H. The specific amino acid requirements of a mammalian cell (strain L) in tissue culture. J. biol. Chem. 1955, 214, 839–852.
7. Ham, R. G. Clonal growth of mammalian cells in a chemically defined, synthetic medium. PNAS 1965, 53, 288.
8. Fürst, P. Old and new substrates in clinical nutrition. J. Nutr. 1998, 128, 789–796.
9. Sánchez-Kopper, A., Becker, M., Pfizenmaier, J., Kessler, C. et al. Tracking dipeptides at work-uptake and intracellular fate in CHO culture. AMB Express 2016, 6, 48.
10. Barrett and Jacobia (2011) EP 2 561 065 B1. Munich: European Patent Office.
11. Pfizenmaier, J., Matuszczyk, J. C., Takors, R. Changes in intracellular ATP-content of CHO cells as response to hyperosmolality. Biotechnol. Prog. 2015, 31, 1212–1216.
12. Buchholz, J., Schwentner, A., Brunnenkan, B., Gabris, C. et al. Platform engineering of Corynebacterium glutamicum with reduced pyruvate dehydrogenase complex activity for improved production of L-lysine, L-valine, and 2-ketoisovalerate. Appl. Environ. Microbiol. 2013, 79, 5566–5575.
13. Henderson, J. W., Brooks, A. Improved amino acid methods using Agilent ZORBAX Eclipse Plus C18 columns for a variety of Agilent LC instrumentation and separation goals. Agilent Technologies, Santa Clara, CA 2010.
14. Teleki, A., Sánchez-Kopper, A., Takors, R. Alkaline conditions in hydrophilic interaction liquid chromatography for intracellular metabolite quantification using tandem mass spectrometry. Anal. Biochem. 2015, 475, 4–13.
15. Feith, A., Teleki, A., Graf, M., Favilli, L. et al. HILIC-enabled (13)C metabolomics strategies: comparing quantitative precision and spectral accuracy of QTOF High- and QQQ low-resolution mass spectrometry. Metabolites 2019, 9, 63.
16. Cserjan-Puschmann, M., Kramer, W., Duerrschmid, E., Striedner, G. et al. Metabolic approaches for the optimisation of recombinant fermentation processes. Appl. Microbiol. Biotechnol. 1999, 53, 43–50.
17. Kanehisa, M., Goto, S. KEGG: Kyoto encyclopedia of genes and genomes. Nucleic. Acids. Res. 2000, 28, 27–30.
18. Hefzi, H., Ang, K. S., Hanscho, M., Bordbar, A. et al. A consensus genome-scale reconstruction of Chinese hamster ovary cell metabolism. Cell Syst. 2016, 3, 434–443.
19. Quek, L. E., Dietmair, S., Krömer, J. O., Nielsen, L. K. Metabolic flux analysis in mammalian cell culture. Metab. Eng. 2010, 12, 161–171.
20. Sheikh, K., Förster, J., Nielsen, L. K. Modeling hybridoma cell metabolism using a generic genome-scale metabolic model of Mus musculus. Biotechnol. Prog. 2005, 21, 112–121.
21. Martens, D. E. Metabolic flux analysis of mammalian cells. Syst. Biol. 2007, 275–299.
22. Franěk, F., Šrámková, K. Protection of B lymphocyte hybridoma against starvation-induced apoptosis: survival-signal role of some amino acids. Immunol. Lett. 1996, 52, 139–144.
23. Cherlet, M., Marc, A. Intracellular pH monitoring as a tool for the study of hybridoma cell behavior in batch and continuous bioreactor cultures. Biotechnol. Prog. 1998, 14(4), 626–638.
24. Becker, M., Junghans, L., Teleki, A., Bechmann, J. et al. Perfusion cultures require optimum respiratory ATP supply to maximize cell-specific and volumetric productivities. Biotechnol. Bioeng. 2019, 116, 951–960.
25. Bulté, D., Palomares, L. A., Ramírez, O. T., Gómez, C. Overexpression of the mitochondrial pyruvate carrier increases CHO cell and recombinant protein productivity and reduces lactate production. In "Cell Culture Engineering XVI", A. Robinson, PhD, Tulane University R. Venkat, PhD, MedImmune E. Schaefer, ScD, J&J Janssen Eds, ECI Symposium Series, (2018).
26. Kilburn, D. G., Lilly, M. D., Webb, F. C. The energetics of mammalian cell growth. J. Cell Sci. 1969, 4, 645–654.
27. Locasale, J. W., Cantley, L. C. Metabolic flux and the regulation of mammalian cell growth. Cell Metab. 2011, 14, 443–451.

SUPPORTING INFORMATION

Additional supporting information may be found online in the Supporting Information section at the end of the article.

How to cite this article: Verhagen N, Wijaya AW, Teleki A, et al. Comparison of L-tyrosine containing dipeptides reveals maximum ATP availability for L-prolyl-L-tyrosine in CHO cells. *Eng Life Sci*. 2020;20:384–394. https://doi.org/10.1002/elsc.202000017